

## Electronic supplementary information (ESI)

# The compression of deformed microgels at an air/water interface

Takahisa Kawamoto,<sup>[a]</sup> Kohei Yanagi,<sup>[a]</sup> Yuichiro Nishizawa,<sup>[a]</sup> Haruka Minato,<sup>[a]</sup> and Daisuke Suzuki<sup>\*[a,b]</sup>

[a] T. Kawamoto, K. Yanagi, Dr. Y. Nishizawa, Dr. H. Minato, Prof. Dr. D. Suzuki  
Graduate School of Textile Science & Technology, Shinshu University, Ueda, Nagano 386-8567, Japan.  
E-mail: d\_suzuki@shinshu-u.ac.jp (D.S.)

[b] Prof. Dr. D. Suzuki  
Research Initiative for Supra-Materials, Interdisciplinary Cluster for Cutting Edge Research, Shinshu  
University, Ueda, Nagano 386-8567, Japan.

## Table of Contents

<b>Experimental Details</b> .....	3-4
Materials	
Microgel synthesis	
Microgel labeling	
Optical-/Fluorescence-microscopy characterization	
Electrical-conductivity-titration characterization	
Atomic-force-microscopy (AFM) characterization	
Electrophoretic-mobility (EPM) characterization	
Characterization of the microgels compressed at the air/water interface	
Microgel-array analysis	
<b>Results and Discussion</b> .....	5-16
Table S1. Chemical composition and characteristics of the microgels used in this study	
Figure S1. Photographs, optical-microscopy images, and histograms of the size distribution of the microgels	
Figure S2. AFM-height images, cross-sectional profiles and AFM-phase images of each microgel	
Figure S3. The array structures of the CS0.60 microgel at the air/water interface over a wide area at 1 mN/m	
Figure S4. The array structures of the CS0.60 microgel at the air/water interface	
Figure S5. Fluorescence-microscopy images of the highly compressed microgels at the air/water interface	
Figure S6. The array structures of the CS0.68 microgel at the air/water interface	
Figure S7. The array structures of the CS0.80 microgel at the air/water interface	
Figure S8. The array structures of the CS0.88 microgel at the air/water interface	
Figure S9. The array structures of the microgels on glass substrates	
Figure S10. Compression isotherms of the microgels at the air/water interface	
Figure S11. AFM-height images and cross-sectional profiles of the CS0.60 microgel	
<b>Supplementary Movies</b> .....	17
<b>References</b> .....	17

## Experimental Details

### Materials

*N*-isopropyl acrylamide (NIPAm, purity 98%), *N,N'*-methylenebis(acrylamide) (BIS, 97%), potassium peroxydisulfate (KPS, 95%), disodium hydrogen phosphate (Na<sub>2</sub>HPO<sub>4</sub>, 99.5%), anhydrous sodium dihydrogen phosphate (KH<sub>2</sub>PO<sub>4</sub>, 99%), potassium chloride (KCl, 99.5%), 1-ethyl-3-(3-dimethylaminopropyl)-carbodiimide hydrochloride (WSC, 98%), hydrochloric acid (HCl), hydroxide solution (NaOH), sodium chloride (NaCl, 99%), methanol (MeOH, 99.8%), and ethanol (EtOH, 99.5%) were purchased from FUJIFILM Wako Pure Chemical Corporation (Japan) and used as received. Fumaric acid (FAc, 99%) was purchased from Sigma-Aldrich and used as received. 5-aminofluorescein (isomer I) was purchased from Tokyo Chemical Industry (Japan) and used as received. Water for all reactions, including the preparation of solutions and dispersions, was distilled and then ion-exchanged (EYELA, SA-2100E1) before use. Glass substrates (Neo Micro Cover Glass, Matsunami Glass Ind., Ltd.) were used after cleaning using 1) ethanol and 2) pure water.

### Microgel synthesis

In order to visualize the individual microgels at the air/water interface using optical/fluorescence microscopy, fluorescein-labeled microgels were prepared. Initially, microgels copolymerized with a charged monomer, fumaric acid, which has carboxy groups capable of chemically binding fluorescent dyes, were synthesized via a conventional precipitation-polymerization method. This polymerization was conducted in an oil bath using a four-necked round-bottom flask (300 mL) equipped with a reflux condenser and a needle for N<sub>2</sub> sparging. First, an aqueous monomer solution (NIPAm, FAc, cross-linker BIS, water 190 mL) was heated at 70 °C at a constant stirring rate (250 rpm) using a mechanical stirrer. Subsequently, the solution was sparged with N<sub>2</sub> for at least 30 min in order to remove the dissolved oxygen from the system, and an aqueous initiator solution (2 mM KPS dissolved in 10 mL of water) was added to initiate the free-radical polymerization. After 4 h, the dispersion was rapidly cooled in a water bath to room temperature in order to terminate the polymerization. The obtained microgel dispersion was purified by centrifugation/redispersion twice using deionized water at a relative centrifugal force (RCF) of ~70,000 g (Avanti J-26S XP. Beckmann Coulter Inc.).

### Microgel labeling

To observe the microgels using fluorescence microscopy, a fluorescent dye, 5-aminofluorescein (isomer I), was chemically bound to the FAc-derived carboxy groups introduced in the microgels through a carbodiimide reaction.<sup>[1]</sup> First, the microgels were dispersed in phosphate-buffered saline (PBS) solution (137 mM NaCl, 2.68 mM KCl, 2 mM KH<sub>2</sub>PO<sub>4</sub>, 10 mM Na<sub>2</sub>HPO<sub>4</sub>) whose pH was adjusted to 7.4 using an HCl solution. Next, 5-aminofluorescein (isomer I) (0.0868 g, 2.5 mM) and WSC (0.0479 g, 2.5 mM) were added in an amount corresponding to 1 molar fraction of the carboxy groups in the dispersion, i.e., 2.5 mM carboxylic groups in 100 mL, respectively. The mixture was stirred with a magnetic stirrer under shading conditions. After at least 18 h, the reaction solution was purified by centrifugation/redispersion with methanol (3 times) to remove the unreacted fluorescent dye and pure water (at least 3 times) to exchange solvent for pure water.

### Optical-/Fluorescence-microscopy characterization

The microgels were examined using optical/fluorescence microscopy (BX53, Olympus). The diameters of the microgels were evaluated by measuring the center-to-center distance between the microgels obtained from the optical-microscopy images of the microgels packed at a critical concentration,  $C^*$ , where the apparent volume fraction  $\phi_{\text{eff}} = 1$ , at room temperature.<sup>[2]</sup> Colloidal crystals of the microgel dispersion were prepared by first heating the dispersion to 50 °C and then sucking it into a borosilicate glass capillary tube (0.1 × 2.0 mm) by capillary interaction, followed by gradual cooling to 25 °C.  $\Phi_{\text{eff}}$  was

calculated from the intrinsic viscosity  $[\eta]$  (mL/g), which was measured at 25 °C using an Ubbelohde viscometer.<sup>[2]</sup>

### **Electrical-conductivity-titration characterization**

The amount of fumaric acid, i.e., carboxylic groups, introduced into the obtained microgels was determined using electrical-conductivity titration. After the dispersion of the microgels was adjusted to a pH > 11 using a 0.1 M NaOH solution, titrations were performed using a 0.1 M HCl solution.

### **Atomic-force-microscopy (AFM) characterization**

The morphology, i.e., the core diameter ( $D_{\text{core}}$ ), core-shell diameter ( $D_{\text{core-shell}}$ ), and full width at half maximum (FWHM), of the microgels was examined using atomic-force microscopy (AFM5200S, Hitachi High-Tech Corporation). The samples for observation were prepared by pulling a glass substrate up through microgels adsorbed at the air/water interface and drying at room temperature.<sup>[3]</sup> Here, microgels were adsorbed at the air/water interface of a water-filled petri dish after spreading a particulate dispersion (water: ethanol = 1:1) on the air/water interface.

### **Electrophoretic-mobility (EPM) characterization**

The electrophoretic mobility (EPM) of the microgels was evaluated using a Zetasizer NanoZS instrument (Malvern, Zetasizer software v. 4.20). The EPM data was calculated from the average of three measurements at 25 °C. The samples were prepared by adding the microgels to solutions adjusted to pH  $\approx$  3 or pH = 11 using 1 mM HCl or NaOH solutions.

### **Characterization of the microgels compressed at the air/water interface**

Compression isotherms at the air/water interface were evaluated using a Langmuir trough (trough dimensions: 140 mm x 680 mm; compressible area: 924 cm<sup>2</sup>; Kyowa Interface Science Co., Ltd.) equipped with a Wilhelmy plate, a chiller set at 25 °C, and a fluorescence-microscopy system (lamp: HBO-100; excitation: 450-490 nm; emission: 510 nm; Axio Scope. A1, Zeiss), whose images and movies were recorded using a CCD camera (Image X Earth Type S-2.0M Ver. 3.1.3, Kikuchi Optical Co, Ltd.). The surface pressure,  $\pi$  (mN/m), of the air/water interface was determined via the Wilhelmy method. After confirming that the interface was clean via blank measurements, microgels dispersed in a mixture of 50 vol% water and 50 vol% ethanol were spread onto the whole area of the air/water interface using a micropipette. After 30 min, evaluation of the compression isotherm at the air/water interface was initiated by moving the equipped trough barrier at a constant speed of 10 cm<sup>2</sup>/min while directly observing the adsorbed microgels at the air/water interface.

In order to transfer the microgel monolayers formed at the air/water interface onto a glass substrate (Neo Micro Cover Glass, Matsunami Glass Ind., Ltd.), the glass substrate was dipped in water before spreading the microgels at the air/water interface and it was then pulled up through the microgel monolayer at the air/water interface. The barrier position was automatically adjusted to maintain the target surface pressure. The pull-up speed was 0.1 cm/min at a vertical angle.

### **Microgel-array analysis**

The array structures of the microgels were analyzed using ImageJ (Version 2.0.0) and Python over a 30  $\mu\text{m}$  x 30  $\mu\text{m}$  area of the images obtained at each surface pressure. To calculate the Fourier-transform (FT) fluorescence-microscopy images of the two-dimensional microgel arrays, the ImageJ software (fast-Fourier-transform (FFT) implementation) was used. The following equation (1) was used to calculate the pair-correlation functions:

$$g(r) = \frac{n(r)}{4\pi r^2 dr \rho} \quad (1)$$

, where  $n(r)$  is the number of particles present over a distance  $r$  to  $r + dr$ , and  $\rho$  is average particle density in the system.

## Results and Discussion

**Table S1.** Chemical composition and characteristics of the microgels

Code	NIPAm / g	BIS / g	FAc / g	Diameter / nm	*Core-Shell ratio	**Deformation ratio	-COOH content / mmol g <sup>-1</sup>	$\mu / 10^{-8} \text{ m}^2 \text{ V}^{-1} \text{ s}^{-1}$		
								Non-Labeling	Labeling	
CS0.60	3.33	0.05	0.35	1650 ± 148	0.60	210	1.42	pH3	-1.25 ± 0.03	-0.68 ± 0.03
								pH11	-2.60 ± 0.04	-2.40 ± 0.03
CS0.68	2.97	0.12	0.35	1567 ± 130	0.68	66	1.57	pH3	-0.67 ± 0.03	-0.81 ± 0.01
								pH11	-2.42 ± 0.02	-2.41 ± 0.02
CS0.80	2.89	0.23	0.35	1142 ± 109	0.80	10	1.56	pH3	-0.88 ± 0.03	-0.93 ± 0.04
								pH11	-2.45 ± 0.05	-2.46 ± 0.04
CS0.88	2.80	0.35	0.35	1034 ± 83	0.88	5	1.65	pH3	-1.07 ± 0.01	-0.86 ± 0.03
								pH11	-2.79 ± 0.04	-2.44 ± 0.04

\*The core-shell ratio was calculated by dividing the core diameter (nm) by the core-shell diameter (nm). These values were obtained from the AFM images in Fig.S2.

\*\*The deformation ratio was calculated by dividing width (nm) by height (nm). The width and height were obtained from the cross-sectional profile constructed from the green line in the height images in Fig.2 and Fig.S2.

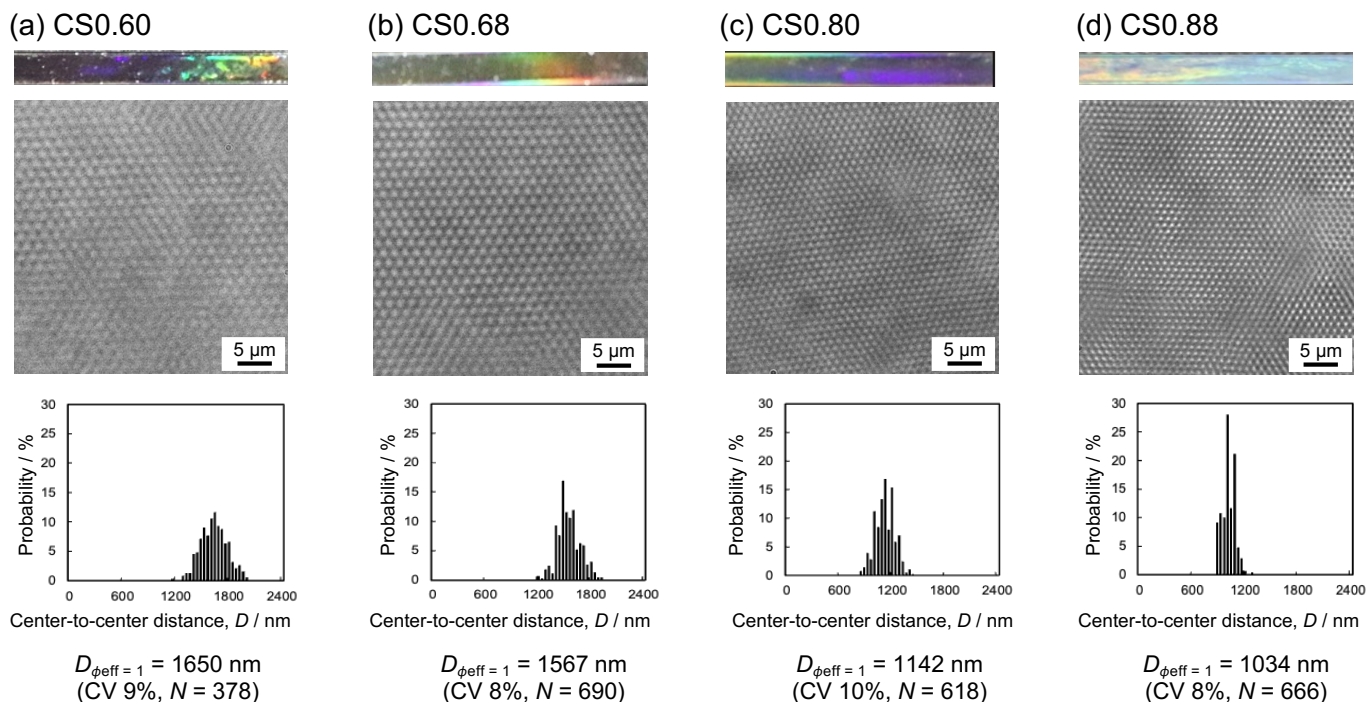
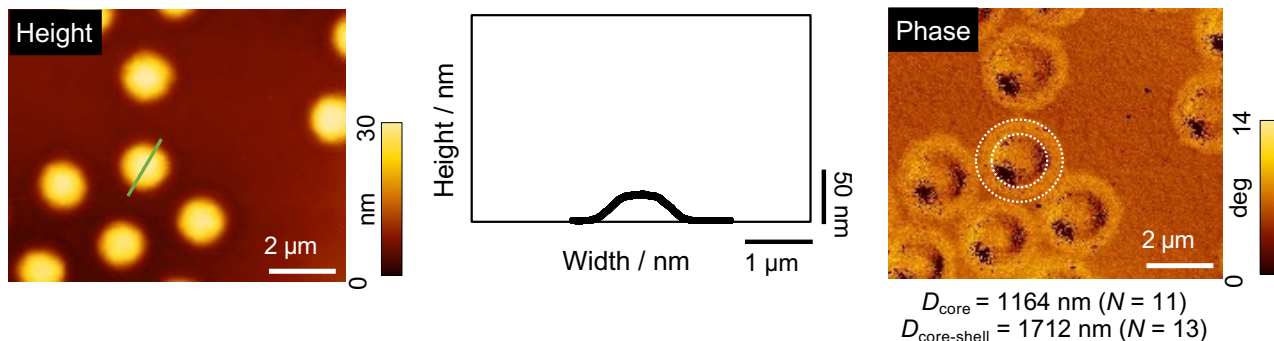
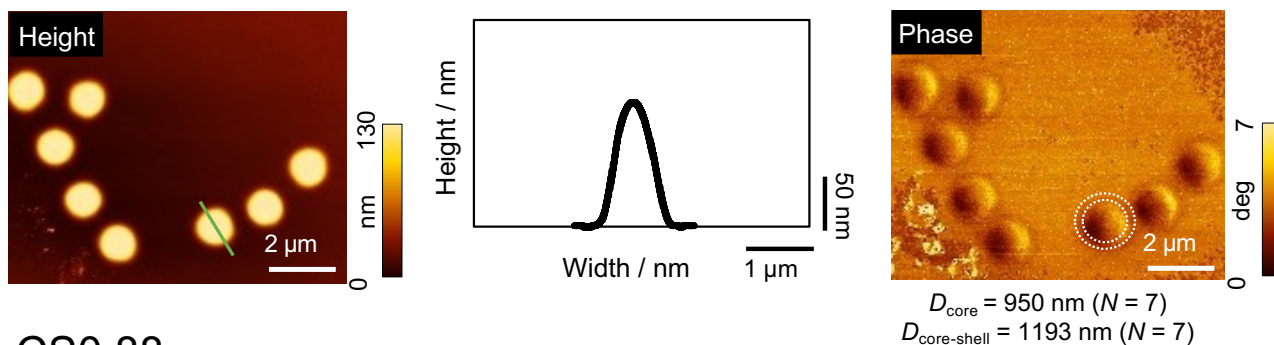


**Fig. S1.** Photographs, optical-microscopy images, and histograms showing the size distribution of colloidal crystals composed of (a) CS0.60, (b) CS0.68, (c) CS0.80, and (d) CS0.88 microgels at the critical concentration,  $C^*$ , where the apparent volume fraction  $\phi_{\text{eff}} = 1$  at room temperature.

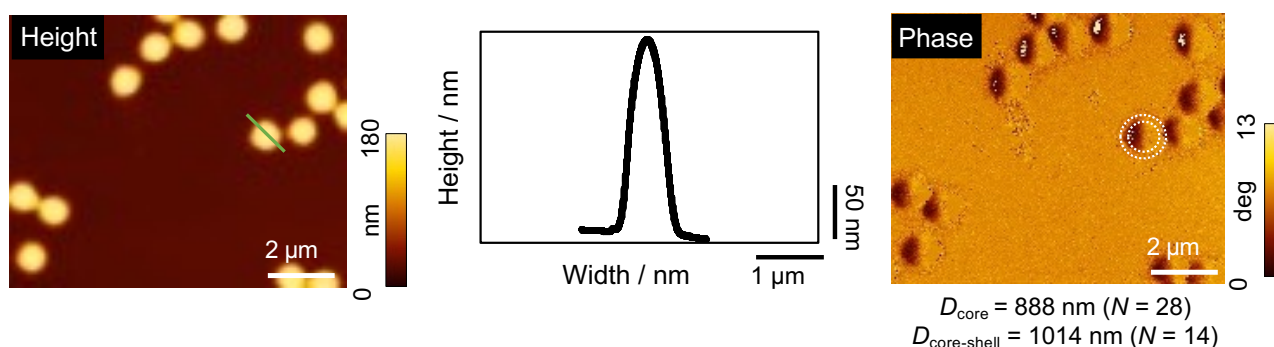
(a) CS0.68



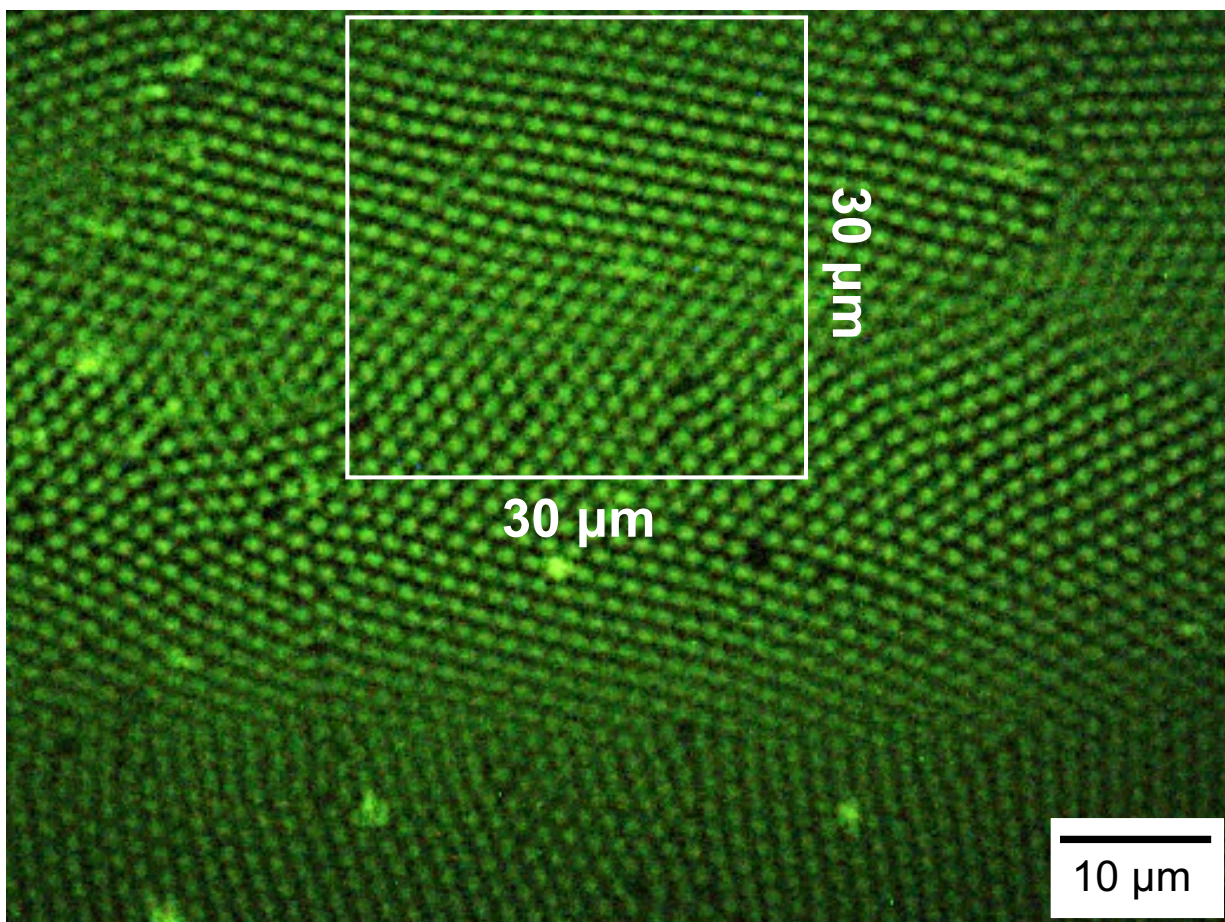
(b) CS0.80



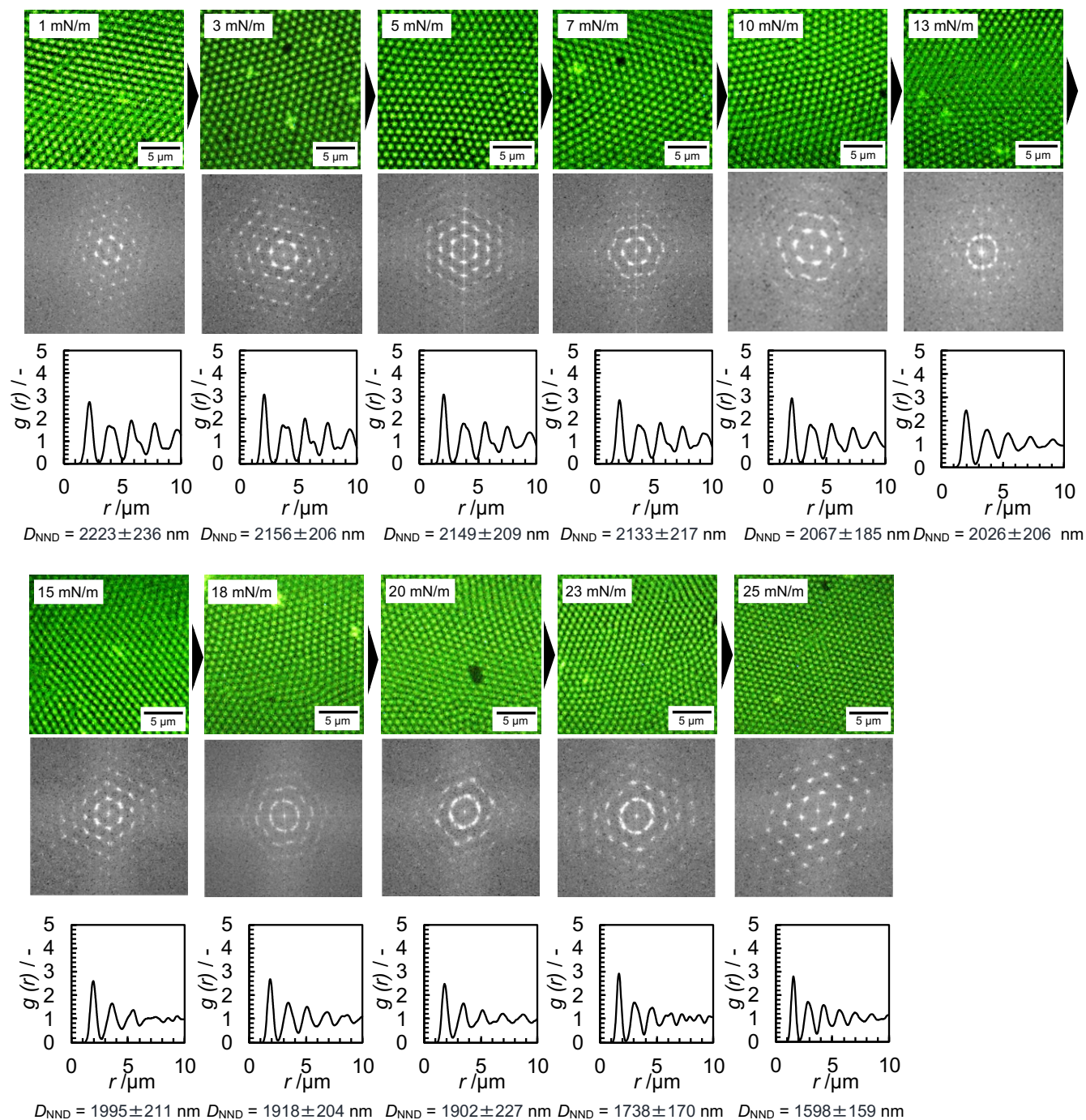
(c) CS0.88



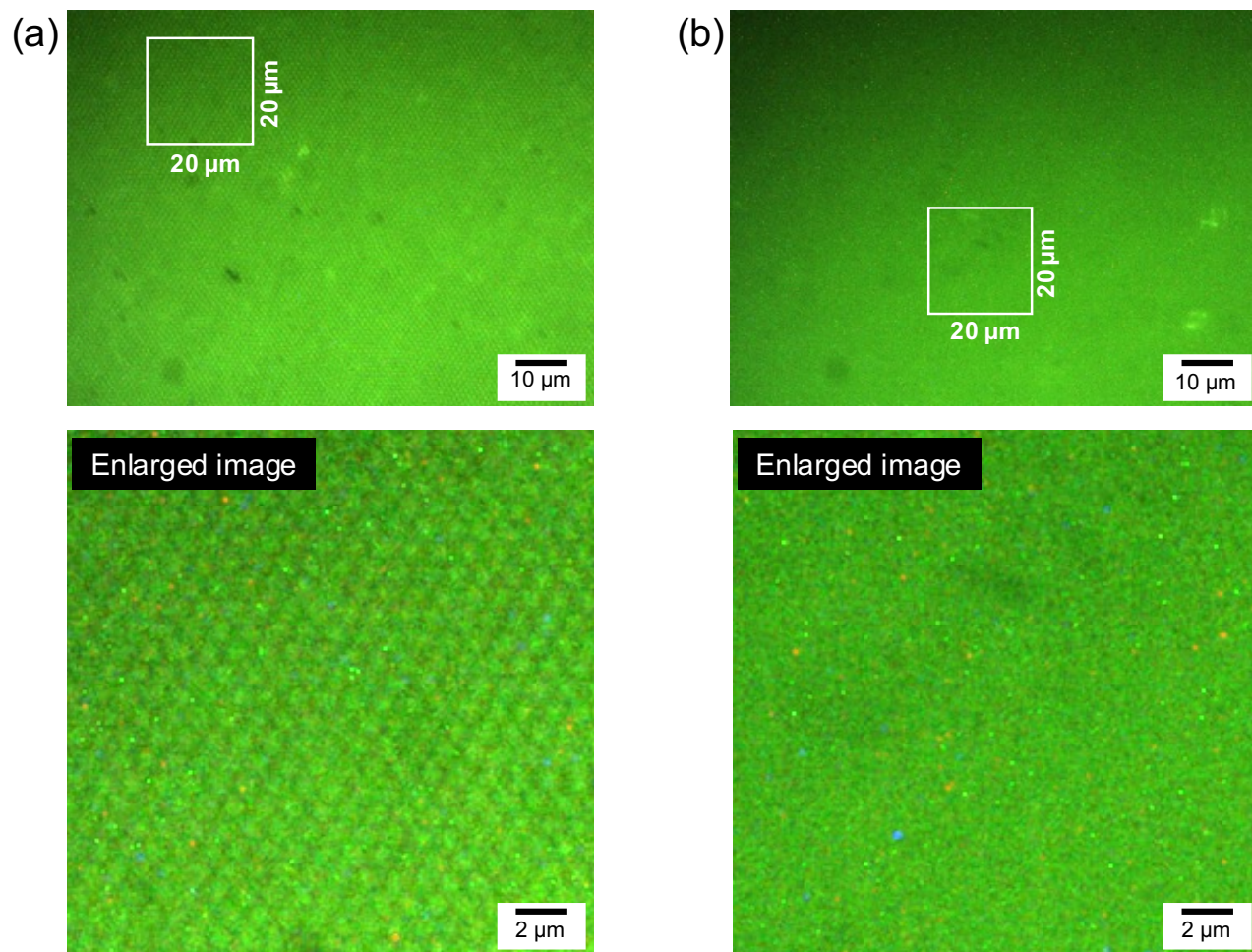
**Fig. S2.** AFM-height image, cross-sectional profile constructed from the height image and the phase image of (a) CS0.68, (b) CS0.80 and (c) CS0.88 microgels deformed on glass substrates. The cross-sectional profiles are constructed from the green line in the height images. The two white circles of different sizes in the AFM phase images represent the core and the core-shell of the microgels.



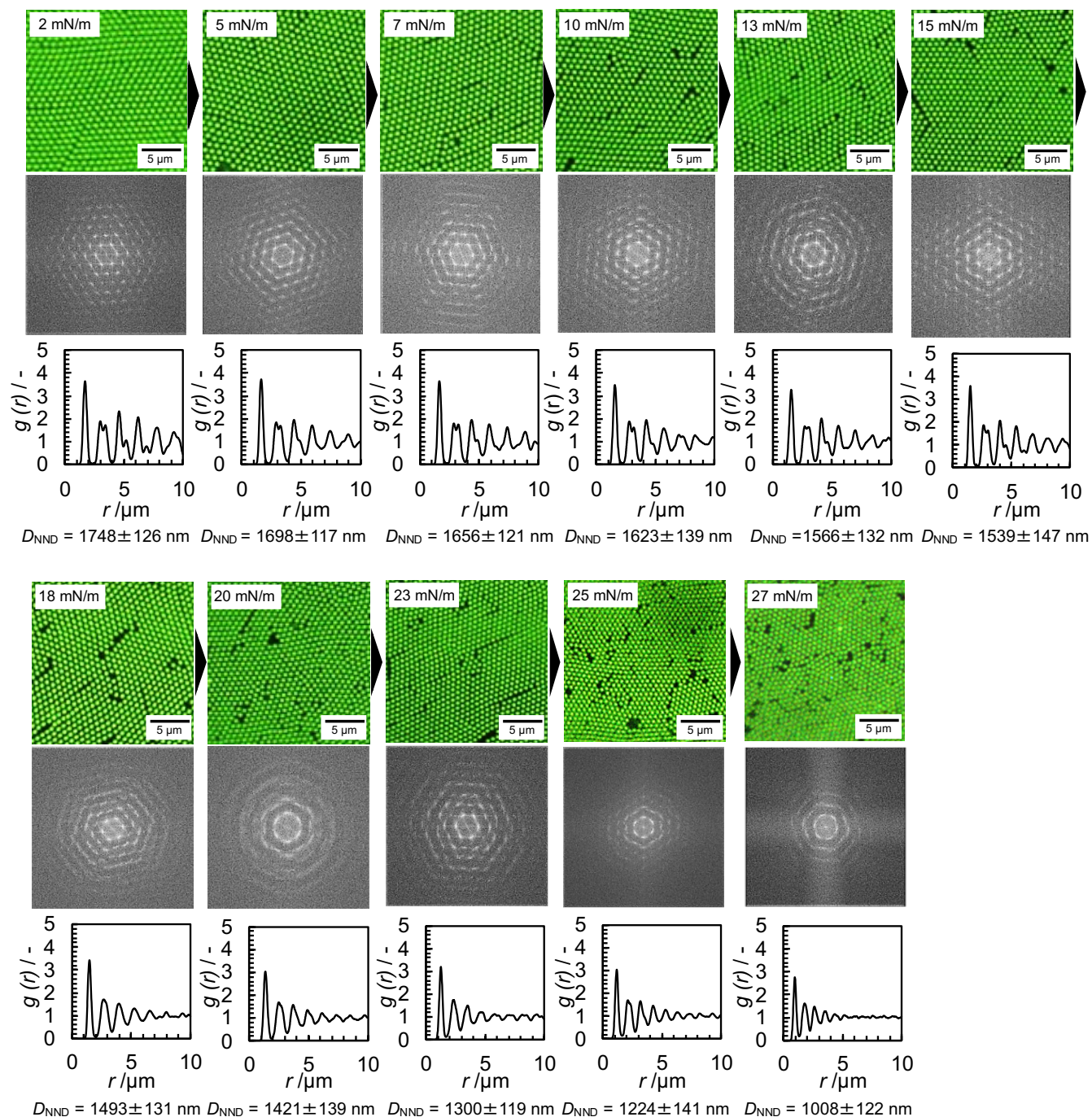
**Fig. S3.** The array structure of the CS0.60 microgel at the air/water interface over a wide area at 1 mN/m. White squares indicate the images used in Fig. 3a.



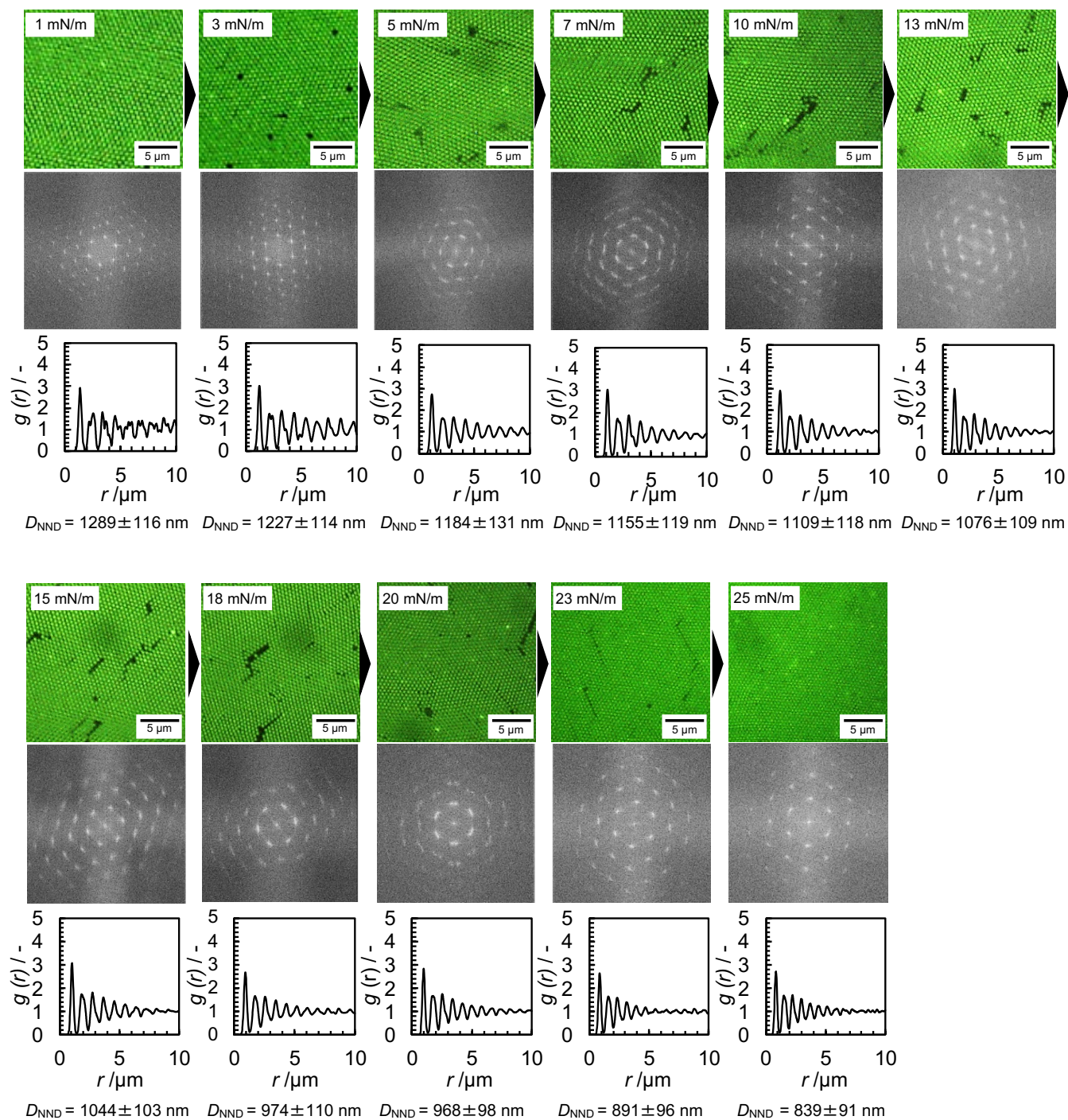
**Fig. S4.** The array structure, FFT images, and the pair-correlation function for the CS0.60 microgels at the air/water interface at different surface pressures,  $\pi$ , obtained using fluorescence microscopy.



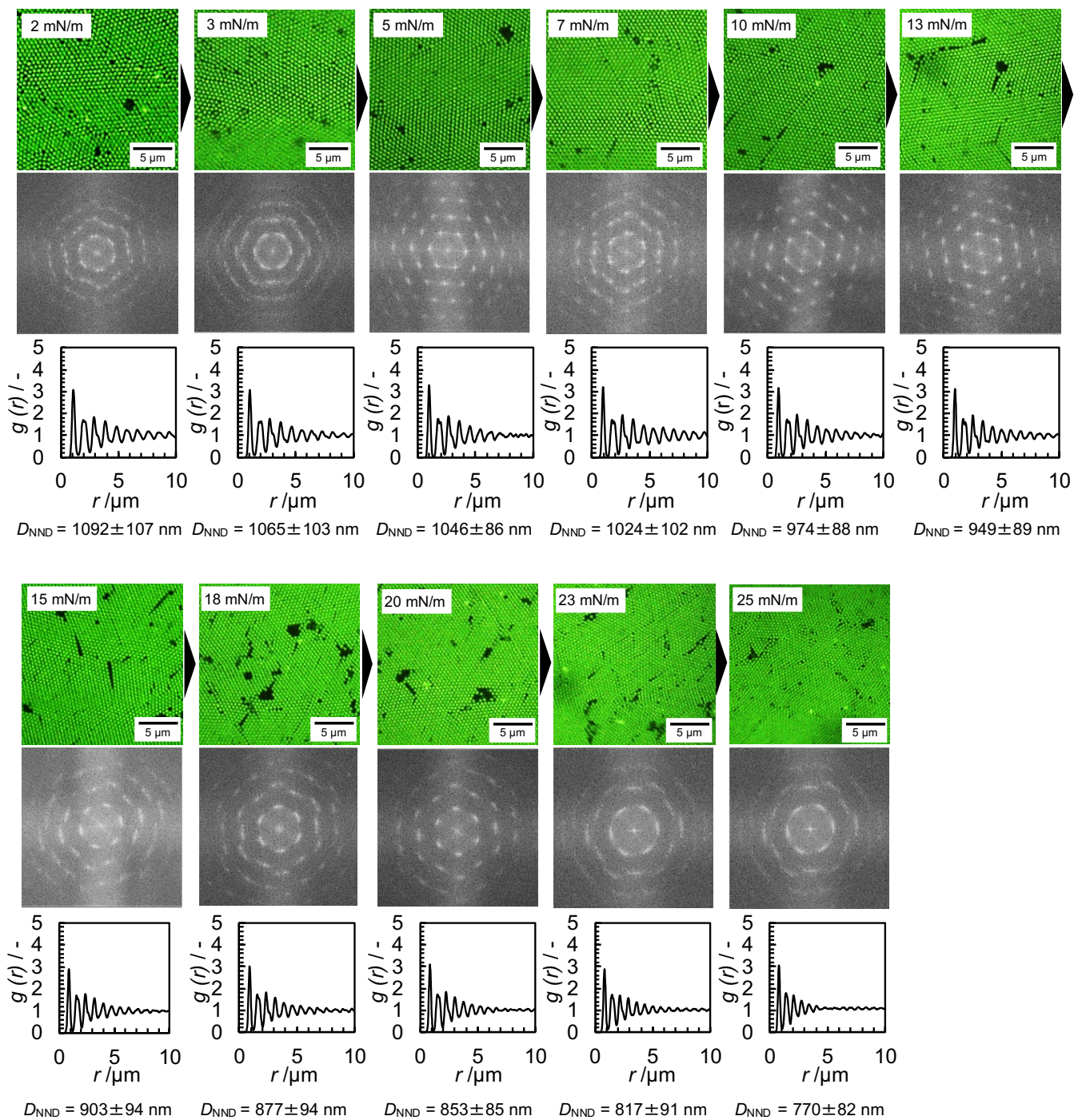
**Fig. S5.** Fluorescence-microscopy images of the CS0.60 microgels adsorbed at the air/water interface in a highly compressed state at (a) 26 mN/m and (b) 27 mN/m. This experiment was conducted by increasing the concentration of the initially dropped microgel dispersion.



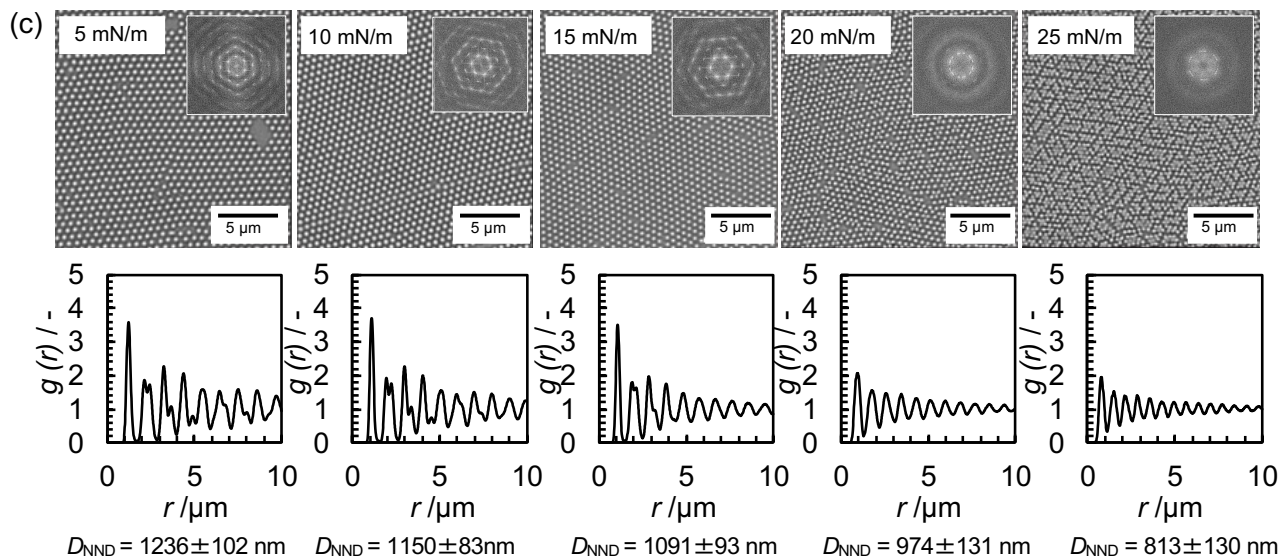
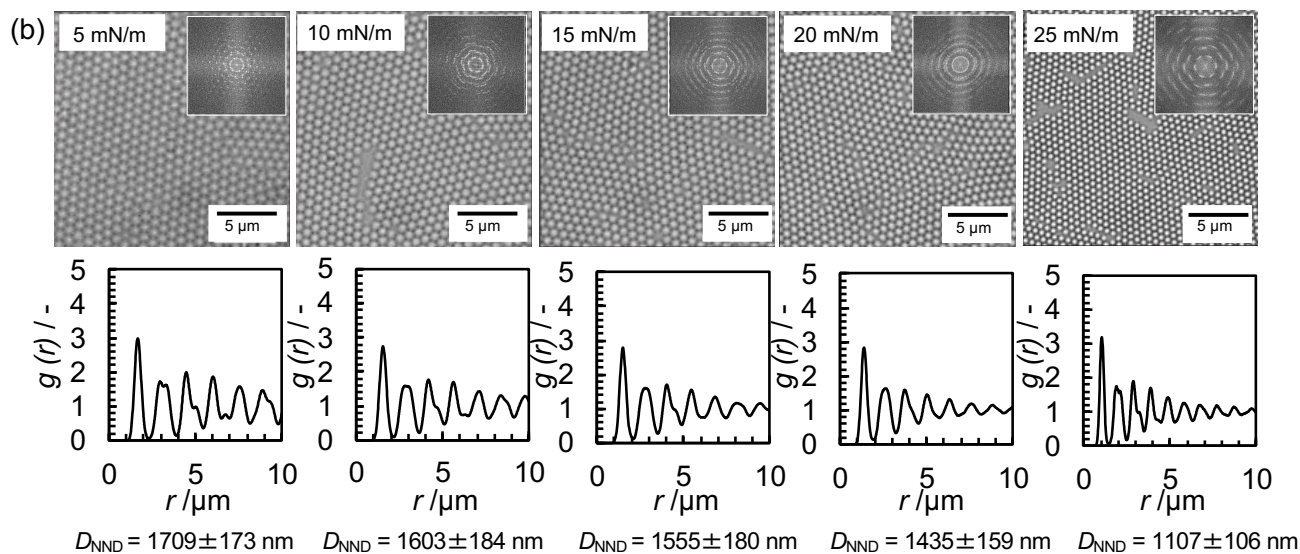
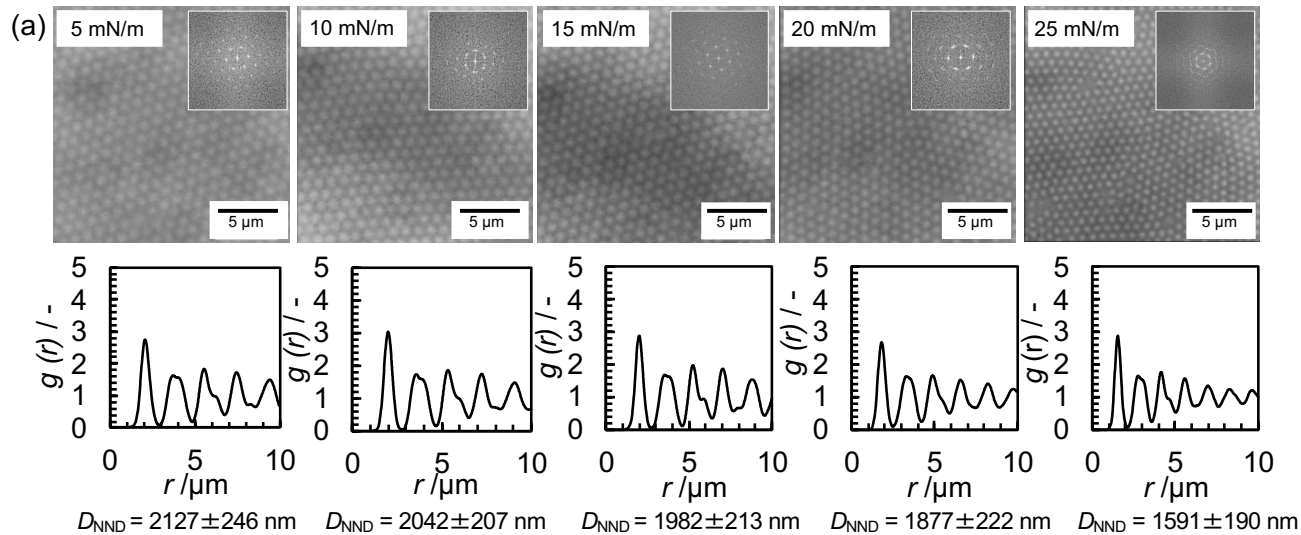
**Fig. S6.** The array structure, FFT images, and the pair-correlation function for the CS0.68 microgels at the air/water interface at different surface pressures,  $\pi$ , obtained using fluorescence microscopy.



**Fig. S7.** The array structure, FFT images, and the pair-correlation function for the CS0.80 microgel at the air/water interface at different surface pressures,  $\pi$ , obtained using fluorescence microscopy.



**Fig. S8.** The array structure, FFT images, and the pair-correlation function for the CS0.88 microgel at the air/water interface at different surface pressures,  $\pi$ , obtained using fluorescence microscopy.



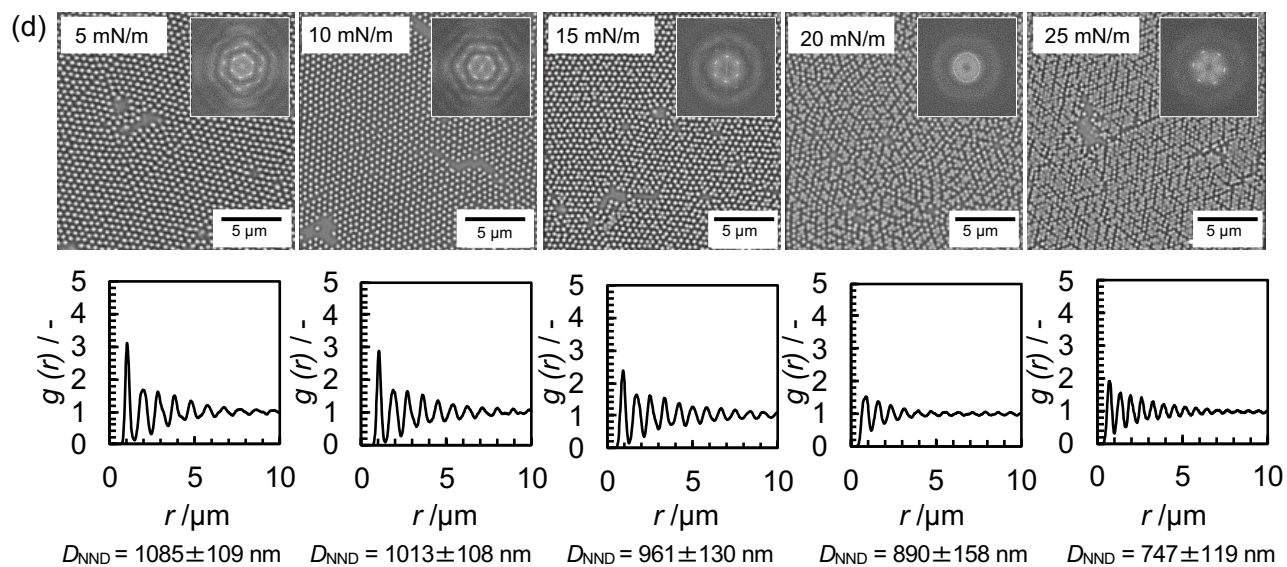


**Fig. S9.** The array structure, FFT images, and the pair-correlation function for the (a) CS0.60, (b) CS0.68, (c) CS0.80, and (d) CS0.88 microgels at the air/water interface at different surface pressures,  $\pi$ , following transfer onto glass substrates obtained from optical microscopy.

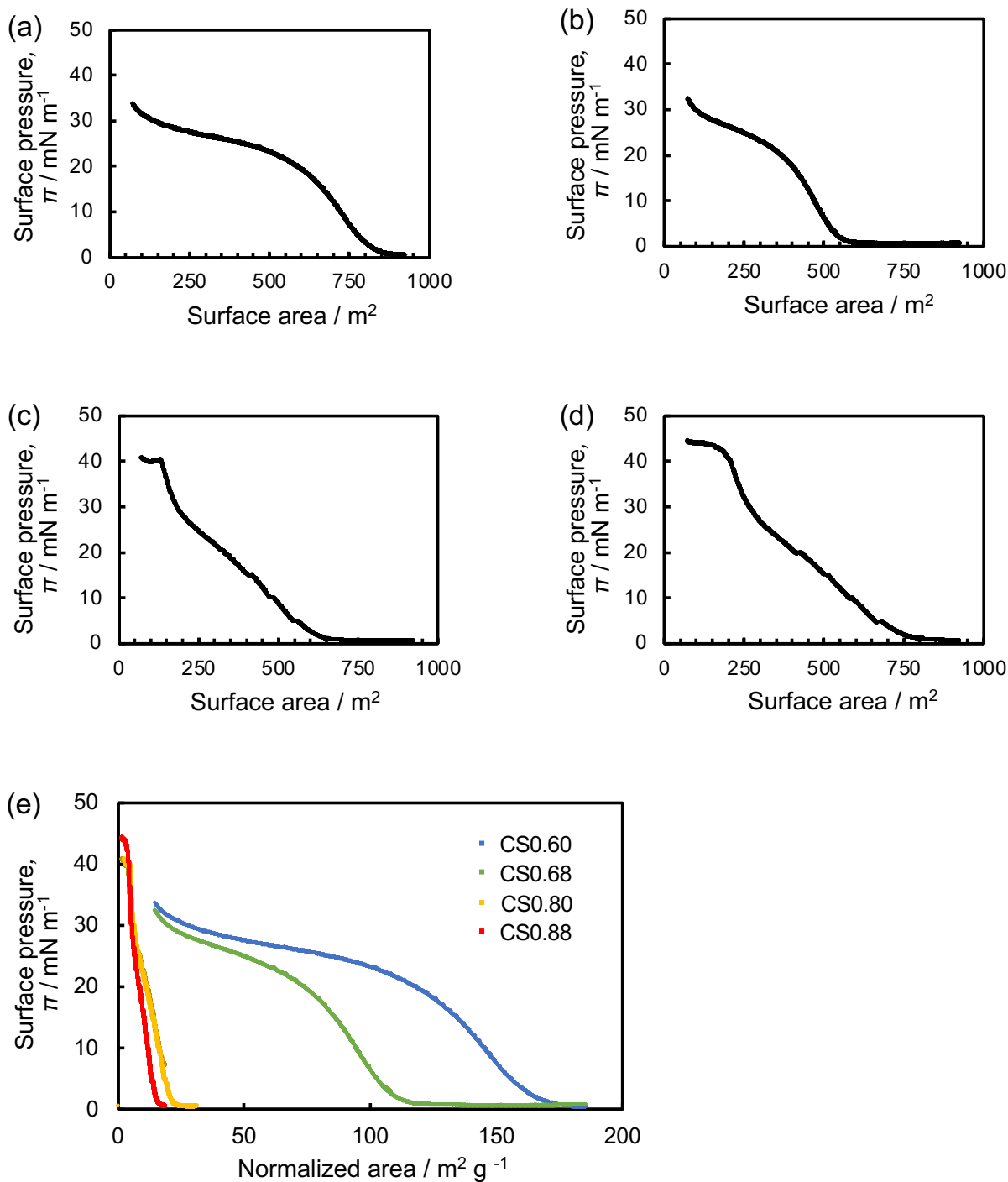


**Fig. S10.** Compression isotherms of the (a) CS0.60, (b) CS0.68, (c) CS0.80, and (d) CS0.88 microgels adsorbed at the air/water interface at a compression speed of 10 cm<sup>2</sup>/min. (e) Surface pressure isotherms as a function of the normalized surface area (= the interfacial area (m) / the quantity of dropped microgels (g)).

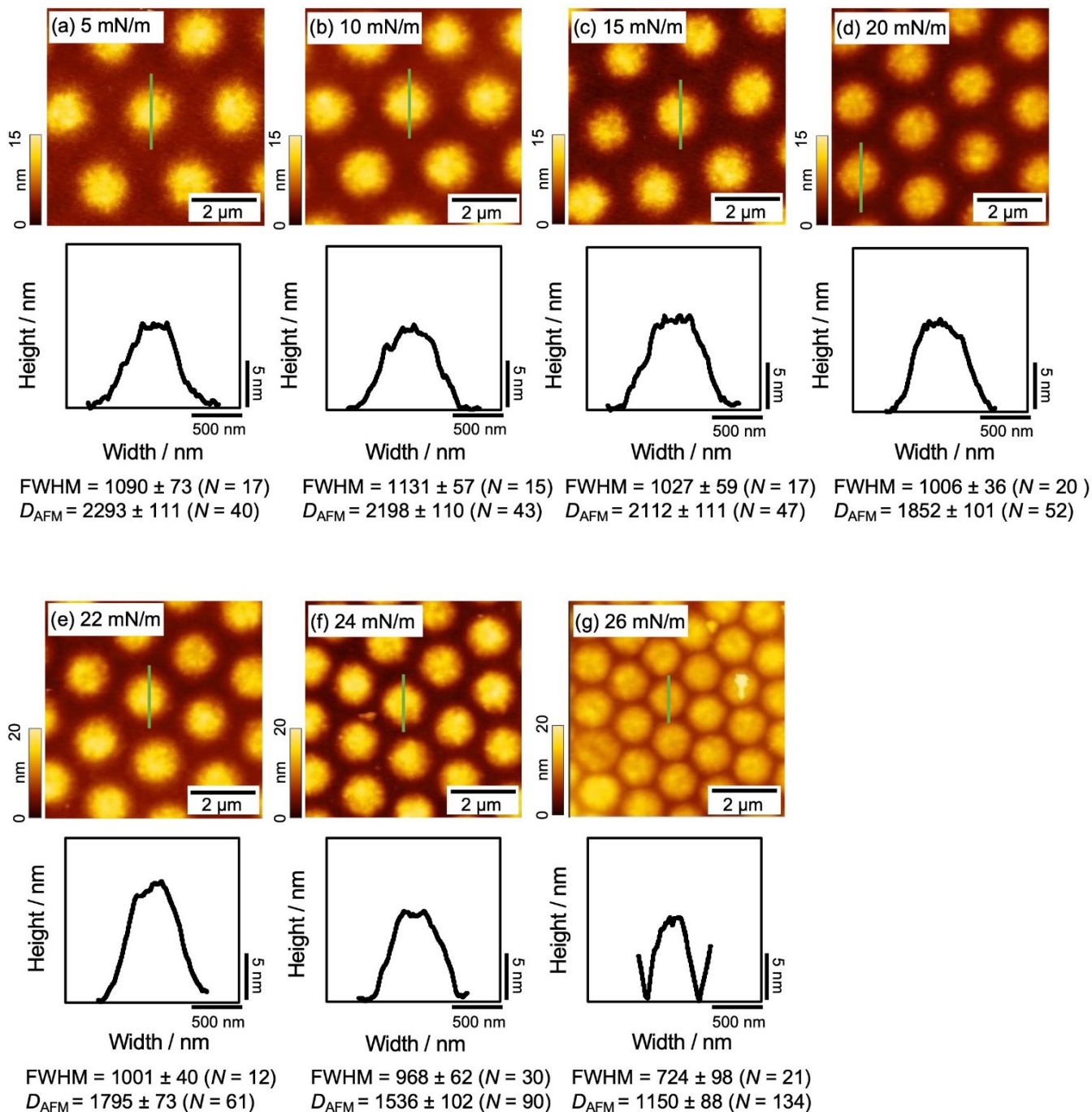


**Fig. S11.** AFM-height images and cross-sectional profiles constructed from the height image of the CS0.60 microgel at (a) 5 mN/m, (b) 10 mN/m, (c) 15 mN/m, (d) 20 mN/m, (e) 22 mN/m, (f) 24 mN/m and (g) 26 mN/m, where microgels adsorbed at the air/water interface were transferred onto glass substrates.

## Supplementary Movies

**Movie S1.** Compression behavior of the CS0.60 microgels adsorbed at the air/water interface when the surface pressure was increased to 4~5 mN/m at a compression speed of 10 cm<sup>2</sup>/min.

## References

- [1] S. Oura, T. Watanabe, H. Minato, D. Suzuki, *KOBUNSHI RONBUNSHU*, 2019, **76**, 226-233.
- [2] K. Urayama, T. Saeki, S. Cong, S. Uratani, T. Takigawa, M. Murai, D. Suzuki, *Soft Matter*, 2014, **10**, 9486-9495.
- [3] T. Watanabe, H. Minato, Y. Sasaki, S. Hiroshige, H. Suzuki, N. Matsuki, K. Sano, T. Wakiya, Y. Nishizawa, T. Uchihashi, T. Kureha, M. Shibayama, T. Takata, D. Suzuki, *Green Chem.*, 2023, **25**, 3418-3424.